



# Normal Radiologic Anatomy and Anatomical Variants of the Chest Relevant to Thoracic Surgery

Cheng Ting Lin and Elliot K. Fishman

## Abstract

Preoperative planning requires the careful review of imaging obtained to define anatomy and determine the optimal approach. Normal anatomy and anatomical variants can be challenging and in select cases may simulate pathology. Understanding the radiologic anatomy of the chest is essential to perform safe and successful surgery. This section focuses on the critical anatomic structures seen on imaging that every thoracic surgeon should recognize.

## Keywords

Normal anatomy · Computed tomography · Aortic arch variants · Tracheobronchial variants · Accessory fissures · Lymph node stations · Adenopathy mimics · Chest wall anomaly · Thoracic nerves

## Abbreviations

CT	Computed tomography
DA	Descending aorta
E	Esophagus
IASLC	International Association for the Study of Lung Cancer
LC	Left carotid
LPA	Left pulmonary artery
LS	Left subclavian
MR/MRI	Magnetic resonance/magnetic resonance imaging
PA	Pulmonary artery
RC	Right carotid
RLN	Recurrent laryngeal nerve
RPA	Right pulmonary artery
RS	Right subclavian
SVC	Superior vena cava
T	Trachea
TNM	Tumor, node, and metastasis

C. T. Lin (✉) · E. K. Fishman  
Department of Radiology and Radiological Science,  
Johns Hopkins University School of Medicine,  
Baltimore, MD, USA  
e-mail: [clin97@jhmi.edu](mailto:clin97@jhmi.edu); [efishman@jhmi.edu](mailto:efishman@jhmi.edu)

**Table 6.1** Examples of thoracic anatomic variants

Vascular
Right aortic arch
Aberrant subclavian artery
Left superior vena cava
Airways
Tracheal bronchus
Cardiac bronchus
Tracheal diverticulum
Lung fissures
Incomplete fissure
Accessory fissure
Azygos fissure
Situs anomalies
Lymph node mimics
Pericardial recess fluid
Pericardial cyst
Thymic cyst
Cisterna chyli
Bone
Cervical rib
Pectus deformity

## 6.1 Vascular

Aortic arch anatomy derives its basis from Edward's hypothetical double-arch model [1], depicted in Fig. 6.1. Separation of the segment between the right subclavian artery takeoff and the descending aorta results in normal anatomy. An aberrant right subclavian artery forms when there is embryological interruption between the two right-sided arch vessels.

Right-sided aortic arch is an aortic arch anomaly resulting from developmental interruption of the left aortic arch. The incidence is approximately 0.1%. Three configurations of the right-sided aortic arch have been described:

- Right aortic arch with aberrant origin of the left subclavian artery (Fig. 6.2)—persistence of the ligamentum arteriosus on the left leads to the formation of a vascular ring
- Right aortic arch with mirror-image branching of the arch vessels—typically associated with cyanotic congenital heart disease
- Right aortic arch with isolation of the left subclavian artery—least common malformation

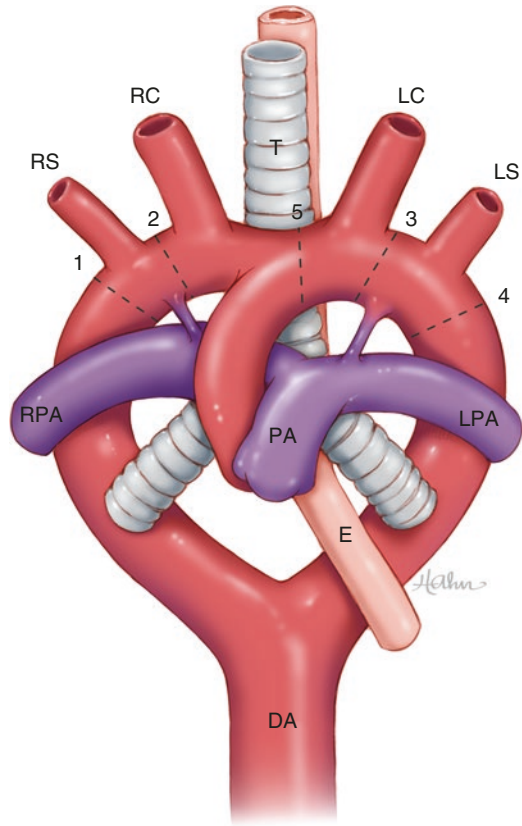


**Fig. 6.1** Illustration of Edward's hypothetical double-arch model. Regression of the right arch at location 1 or 2 results in a left arch without or with an aberrant right subclavian artery, respectively. Alternatively, obliteration of the left arch at segment 3 or 4 gives rise to a right arch with or without an aberrant left subclavian artery, respectively

On frontal chest radiograph, the right arch is directly visualized as a vascular silhouette causing slight leftward deviation of the trachea. The right aortic arch reaches a relatively high position along the mediastinum compared to the left aortic arch. The descending aorta is positioned on the right side. Patients with incidentally detected right arch may require additional cross-sectional imaging to evaluate for congenital heart disease or a vascular ring.

Aberrant origin of the subclavian artery originates from the distal aortic arch and generally follows a retrosophageal course. Its incidence varies from 0.5% to 2%, with a higher association with right-sided arch than left-sided arch. The anomalous subclavian artery is

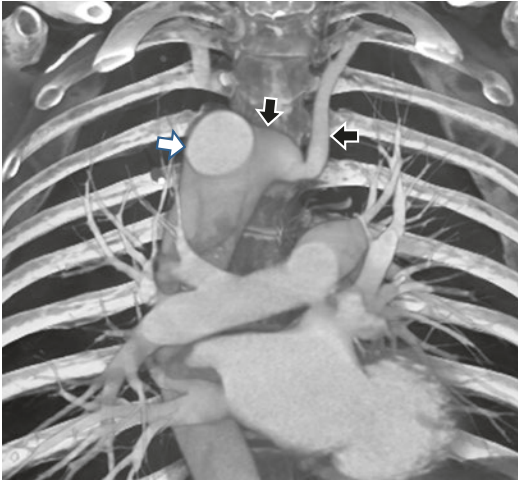


**Fig. 6.2** Volume-rendering technique image demonstrating aberrant origin of the left subclavian artery (*black arrows*) with a diverticulum of Kommerell at its origin from the right-sided aortic arch (*white arrow*). The aberrant left subclavian artery is the last branch to arise from the aortic arch and courses between the esophagus and vertebral bodies

readily seen on CT or MR imaging (Fig. 6.2). Kommerell's diverticulum is an aneurysmal dilation of the most proximal portion of the aberrant subclavian artery. While most patients with this anomaly are asymptomatic, occasionally patients can develop swallowing difficulty termed dysphagia lusoria. Rare presentations include rupture or dissection of a diverticulum of Kommerell.

The persistent left superior vena cava (SVC) is a congenital venous anomaly that arises from failure of the left anterior cardinal vein to obliterate during embryological development. It occurs in ~0.4% of the general population and ~5% of those with congenital heart disease. In most cases (82–90%) of persistent left SVC, the right-sided SVC is present and decreased in caliber compared to normal. The persistent left SVC drains into a dilated coronary sinus in 92% of the cases, whereas it terminates at the left atrium in 8% of the cases resulting in a right-to-left shunt which is usually not clinically significant. Cases of persistent left SVC are typically diagnosed during line placement or incidentally during chest CT exams (Fig. 6.3). Patients are usually asymptomatic in the absence of concomitant congenital heart disease.



**Fig. 6.3** Volume-rendering technique image showing a persistent left SVC (*white arrow*) draining into the coronary sinus (not shown) as well as a normal right-sided SVC (*black arrow*). No bridging brachiocephalic vein is present between the two SVC

## 6.2 Airways

### 6.2.1 Normal Tracheobronchial Anatomy

The tracheobronchial tree divides in a predictable pattern with occasional variations [2]. The carina is normally at the level of T4–T5. The right mainstem bronchus comes off the trachea at a more vertical angle compared to the left mainstem bronchus. The bronchial segments are named per their corresponding pulmonary segments (Fig. 6.4). Visceral pleura envelopes each pulmonary lobe, except at the pulmonary hilum or when there is an incomplete interlobar fissure. The trilobed right lung is made up of the right upper, right middle, and right lower lobes. The bilobed left lung is made up of the left upper and left lower lobes.

The right upper lobe bronchus is an eparterial bronchus, meaning that it arises from the mainstem bronchus adjacent to or above the corresponding pulmonary artery. It further divides into the apical, anterior, and posterior segmental bronchi. The bronchus intermedius is the segment from the right upper lobe bronchus takeoff to the bifurcation of the right middle and right lower lobe

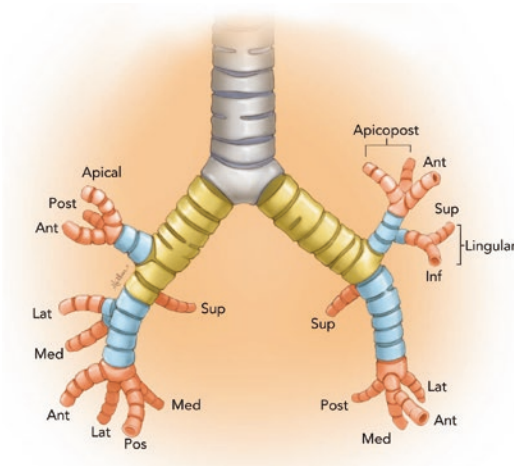


**Fig. 6.4** Illustration of the lobar and segmental bronchial anatomy

bronchi. The right middle lobe bronchus divides into the medial and lateral segmental bronchi. The first branch to come off the bronchus intermedius is normally the bronchus to the right lower lobe superior segment, which projects posteriorly. The remaining four basal segmental bronchi of the right lower lobe have variable division patterns.

The left upper lobe bronchus is normally hyparterial and originates below the left pulmonary artery. The upper portion of the left upper lobe (analogous to the right upper lobe) is divided into the apicoposterior and anterior segments. The lower portion of the left upper lobe (analogous to the right middle lobe) is termed the lingular lobe which is divided into the superior and inferior segments. Like its right-sided counterpart, the bronchus to the left lower lobe superior segment comes off the left lower lobe bronchus before the basal segmental branches. The anterior and medial basal segmental bronchi of the left lower lobe often share a common origin from the lobar bronchus; therefore, they could be considered as the anteromedial segmental bronchus instead.

### 6.2.2 Tracheal Bronchus

A tracheal bronchus represents a variant bronchus arising from trachea and supplying the

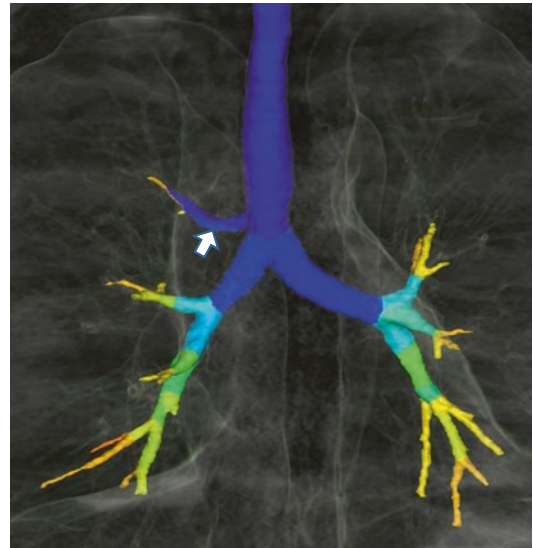


**Fig. 6.5** Virtual bronchoscopy image demonstrating a tracheal bronchus (*arrow*) supplying the right upper lobe

ipsilateral upper lobe [3]. The variant mostly occurs on the right side with a prevalence of 0.1–1.3%. It can supply the entire right upper lobe (Fig. 6.5)—whereby the term “pig bronchus” or “bronchus suis” is sometimes applied—or a segment/subsegment of the right upper lobe. Tracheal bronchi are for the most part incidentally detected on CT or bronchoscopy. Adult patients with tracheal bronchus are generally asymptomatic. Recurrent pneumonia, stridor, and respiratory distress in children with tracheal bronchus have been reported. The tracheal bronchus is also susceptible to blockage during endotracheal intubation.

### 6.2.3 Cardiac Bronchus

Cardiac bronchus is an accessory bronchus originating from the inferomedial aspect of the right main bronchus or bronchus intermedius. The cardiac bronchus courses medially towards the heart (hence its name) in a direction opposite to the right upper lobe bronchus (Fig. 6.6). Its frequency ranges from 0.09% to 0.5%. Accessory cardiac bronchus can be blind-ending or terminates in vestigial parenchymal tissue. They may

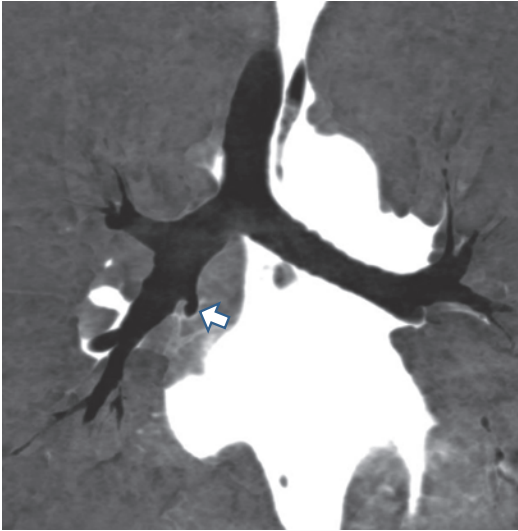


**Fig. 6.6** Minimum intensity projection image of a patient with an incidentally detected accessory cardiac bronchus (arrow)

be a potential reservoir for infectious material which can lead to pneumonia or hemoptysis. Patients with recurrent pneumonia due to an accessory cardiac bronchus may benefit from surgical treatment.

### 6.2.4 Tracheal Diverticulum

Tracheal diverticulum is a paratracheal air cyst with a narrow, often imperceptible, connecting stalk [4]. It occurs in approximately 1% of the general population. The tracheal diverticulum is most commonly located in the thoracic inlet at the right posterolateral aspect of the trachea (Fig. 6.7). Tracheal diverticulum can be acquired in the setting of chronic cough (e.g., chronic obstructive pulmonary disease) secondary to increased intraluminal pressure and resulting herniation of membrane. Thin-section CT is helpful for distinguishing tracheal diverticulum from pneumomediastinum and apical blebs or bullae. Although it is typically a benign incidental finding, symptomatic cases have been reported and attributed to infected secretions within the diverticula.

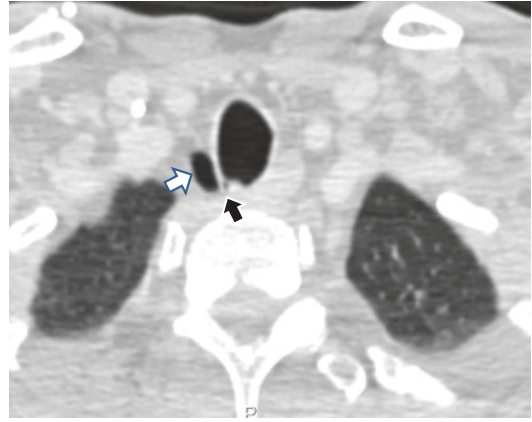


**Fig. 6.7** Axial CT image in lung window showing a tracheal diverticulum (white arrow) with a small thin connection (black arrow) to the posterolateral aspect of the trachea

## 6.3 Fissures

### 6.3.1 Normal and Variant Pulmonary Fissures

Lung fissures are made up of two layers of visceral pleura that form the boundaries of lobar anatomy [5]. Incomplete fissures are common and do not extend all the way to the mediastinum or hilum, allowing pulmonary infections and tumors to cross fissures. On frontal chest radiograph, only the minor (horizontal) fissure separating the right upper and middle lobes can be visualized. The lateral chest radiography shows the major (oblique) fissure extending from the anterior diaphragm to the third–fifth thoracic vertebrae, separating the upper and lower lobes on the left and upper lobe from the middle/lower lobes on the right.

Accessory fissures are common developmental variants in patients with otherwise normal pulmonary anatomy [6], as shown in Fig. 6.8. Accessory fissures are generally incomplete. Common accessory fissures include the left minor fissure, inferior accessory fissure, and superior accessory fissure. A left minor fissure divides the lingular lobe from the left upper lobe proper. The inferior accessory fissure extends in

a cranial direction from the diaphragmatic pleura. The superior accessory fissure lies between the superior and basal segments of the lower lobe.

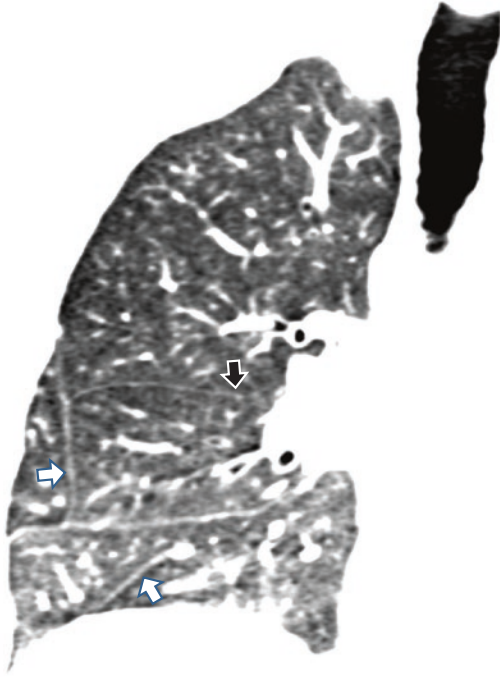


**Fig. 6.8** Coronal CT image showing two accessory fissures (*white arrows*) and an incomplete right minor fissure (*black arrow*)

### 6.3.2 Azygos Fissure

The azygos fissure is the result of embryological migration of the posterior cardinal vein—precursor to the azygos vein—into the upper lobe, typically on the right. The portion of the lung bordered laterally by the azygos fissure is called the azygos lobe (Fig. 6.9a). This anatomic variant occurs in 0.5–1% of the population. Unlike other fissures, the azygos fissure contains a total of four layers of pleura—two layers each of visceral and parietal pleura. The azygos lobe represents partial separation of a normal upper lobe rather than a supernumerary lobe. Unawareness of its presence can lead to technical difficulties during video-assisted thoracic sympathectomy. Displacement of the azygos vein from the azygos fissure to the mediastinum can occur during thoracic surgery, resulting in an “empty azygos fissure” (Fig. 6.9b).

### 6.3.3 Situs Anomalies

Thoracic situs can be grouped into three categories: situs solitus (normal), situs ambiguus (heterotaxy), and situs inversus totalis [7]. Heterotaxy syndromes are abnormal embryological arrangement of the thoracoabdominal viscera, classically divided into bilateral right-sidedness (asplenia)

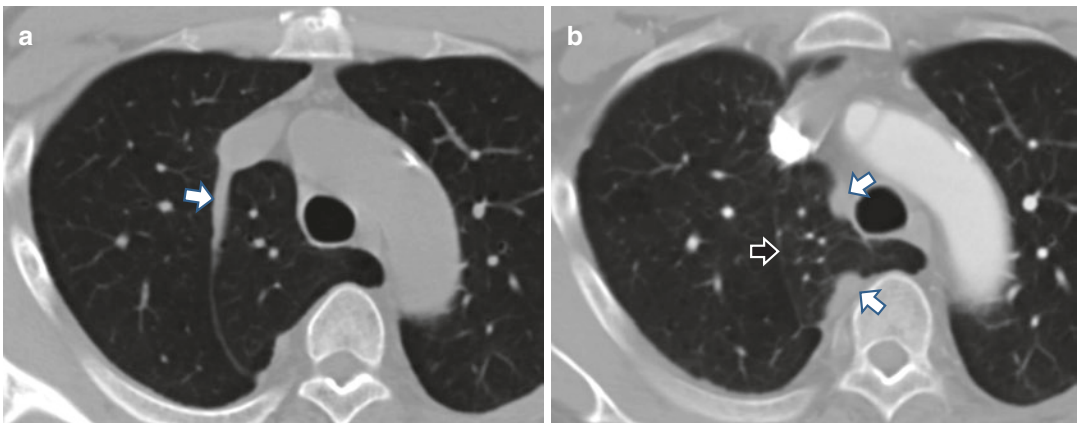


**Fig. 6.9** An azygos fissure containing the azygos vein (*arrow*) was identified on preoperative CT (**a**). CT exam performed after video-assisted thoracic surgery shows

that the azygos vein (*white arrows*) has migrated from the azygos fissure to the medial mediastinum, resulting in an empty azygos fissure (*black arrow*) (**b**)

and bilateral left-sidedness (polysplenia). Bronchial anatomy is a reliable indicator of thoracic situs. The typically left-sided trilobed lung is associated with an eparterial bronchus and a minor fissure, while the bilobed lung is associated with a hyperarterial bronchus and no minor fissure (Fig. 6.10).

## 6.4 Lymph Nodes

### 6.4.1 Nodal Station Map

Accurate staging of thoracic nodes requires use of the International Association for the Study of Lung Cancer (IASLC) lymph node map [8]. This nodal classification system is an essential component of the 7th edition of the tumor, node, and metastasis (TNM) classification of lung cancer published in 2009. Each of the 14 lymph node stations is bounded anatomically by structures best identified on thoracic CT scans (Fig. 6.11).



**Fig. 6.10** Coronal CT image of a patient with two left-sided fissures (*white arrows*) and one right-sided fissure, representing trilobed left lung and bilobed right lung, respectively. Also note the eparterial bronchus on the left side (*black arrow*) which is typically found on the right. Findings are consistent with situs inversus totalis

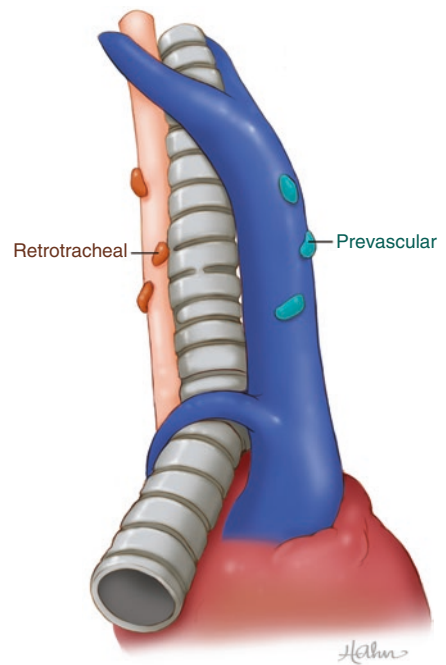
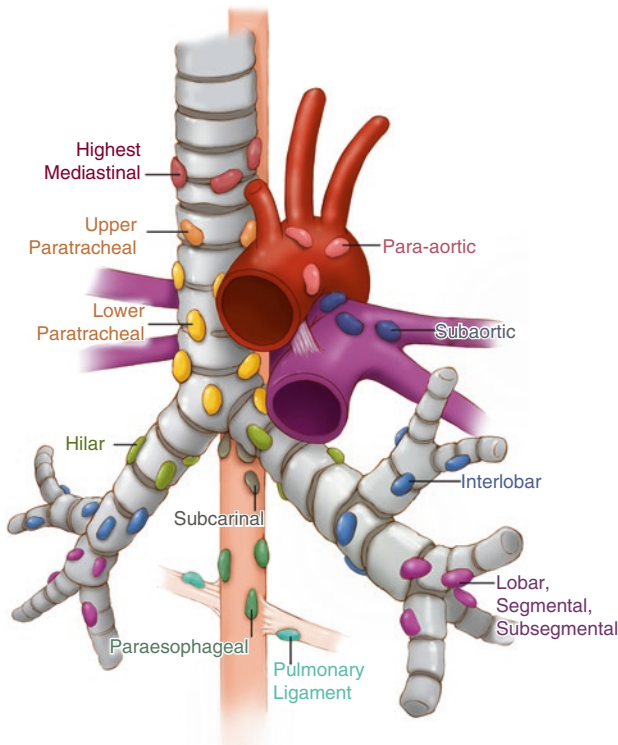


**Fig. 6.11** Illustration of the IASLC lymph node map

Level 1 (supraclavicular) nodes are just above the level of the clavicles. Superior mediastinal nodes consist of the level 2 (right and left upper paratracheal), 3 (prevascular or retrotracheal), and 4 (right and left lower paratracheal) nodes. Level 5 (subaortic) and 6 (para-aortic) nodes are aortic nodes due to their proximity to the aorta. Level 7 (subcarinal), 8 (paraesophageal), and 9 (pulmonary ligament) nodes occupy the inferior mediastinum. N1 nodes by the 7th edition TNM classification consist of level 10 (hilar), 11 (interlobar), 12 (lobar), 13 (segmental), and 14 (subsegmental) nodes.

### 6.4.2 Mimics of Adenopathy

Pericardial recess fluid is a common mimicker of mediastinal adenopathy [9]. The visceral pericardium adheres to the heart and great vessels, forming recesses and sinuses where fluid can accumulate (Fig. 6.12a). Pericardial recesses arise from pericardial cavity proper, transverse sinus, or oblique sinus. Pericardial cavity proper gives rise to the bilateral pulmonic vein and postcaval recesses. The transverse sinus lies posterior to ascending aorta and main pulmonary artery, giving rise to the superior aortic, inferior aortic, and bilateral pulmonic recesses. The oblique sinus is located between the left atrium and the esophagus, and gives rise to the posterior pericardial recess. On CT/MR imaging, pericardial recess fluid measures fluid attenuation, does not demonstrate contrast enhancement, is crescentic or lenticular in shape, and communicates with other pericardial recesses.

Pericardial cyst is a benign cystic lesion adherent to the pericardium [10]. It is considered a developmental defect due to the persistence of a blind-ending parietal pericardial recess. Pericardial cysts are found at the right cardiophrenic angle in 80% of the cases, but can appear anywhere along the pericardium. Cross-sectional imaging typically shows a well-circumscribed unilocular mass with homogeneous fluid density (Fig. 6.12b), without internal septations or enhancement. Its walls are rarely calcified. Most

pericardial cysts are asymptomatic and can be monitored, whereas cyst aspiration or resection should be considered for symptomatic cases (e.g., chest pain or cough).

Thymic cysts are rare anterior mediastinal masses derived from the thymus. The congenital form may develop from a patent thymopharyngeal duct. An acquired thymic cyst can form because of an inflammatory process. They present on imaging as unilocular or multilocular well-circumscribed cystic structures (Fig. 6.12c). Internal soft-tissue attenuation on CT may be due to proteinaceous debris or hemorrhage.

The cisterna chyli is a dilated lymphatic sac located anterior to the L1–L2 vertebrae [11, 12]. It represents the confluence of the thoracic duct and abdominal lymphatic channels. The cisterna chyli is identified on CT by a retrocrural ovoid structure with fluid attenuation (mean of 4–5 Hounsfield units) and no contrast enhancement. Continuity with the thoracic duct is considered diagnostic (Fig. 6.12d). While the cisterna chyli is a part of normal anatomy, it can potentially be misdiagnosed as an enlarged retrocrural lymph node.

---

## 6.5 Bones

### 6.5.1 Chest Wall Anatomy

The osseous components of the chest wall consist of the sternum, 12 pairs of ribs, and thoracic vertebrae [13]. During inspiration, the sternum moves forward and the ribs elevate. The upper seven ribs are called true ribs because they directly articulate with the sternum, while the eighth through tenth ribs are called false ribs as their cartilage is joined together forming the costal arch. The two lowermost ribs lack any attachment to the sternum. The intercostal spaces, the zone between ribs, are held together by the internal and external intercostal muscles. The intercostal neurovascular bundle runs along the caudal groove of the ribs. Caution is warranted to avoid injury to these structures during thoracoscopy and other thoracic procedures that use intercostal space access.

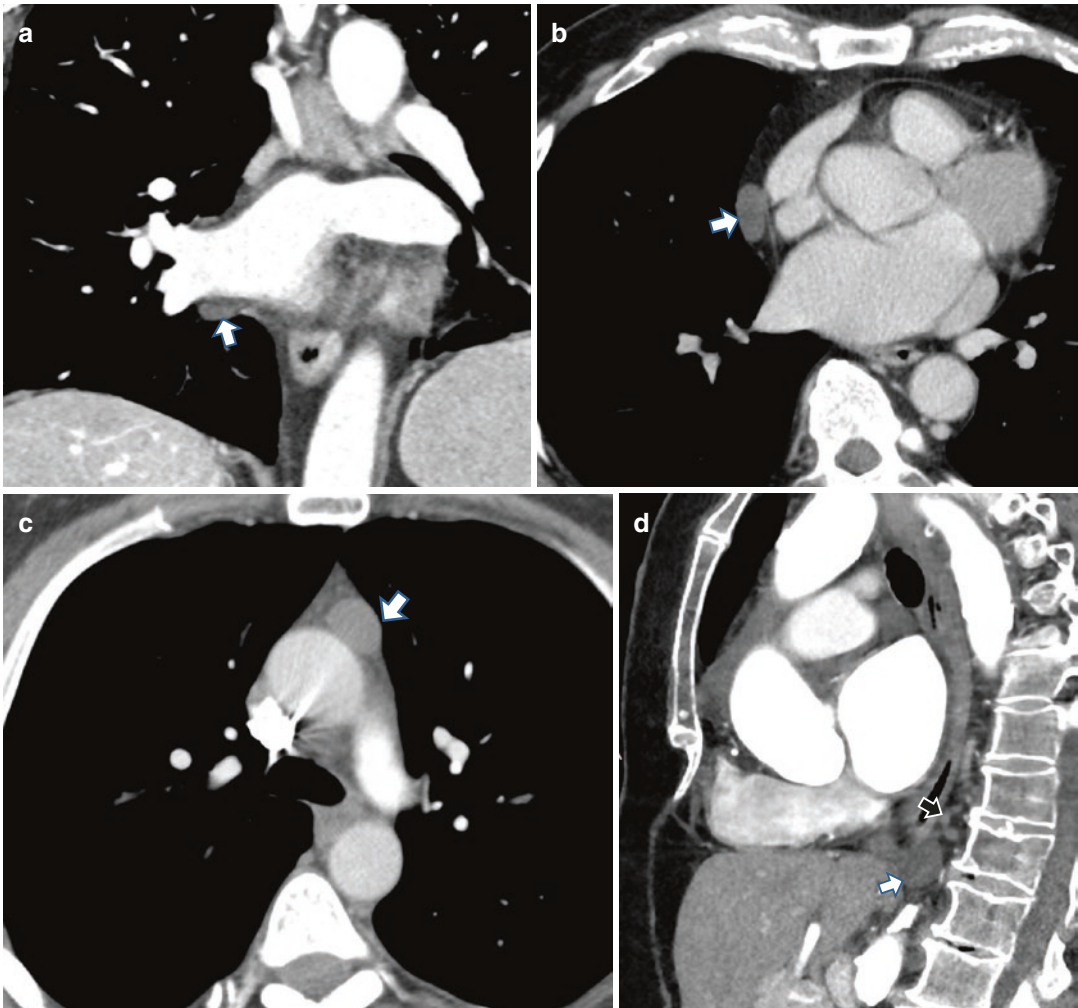


**Fig. 6.12** Mimics of adenopathy. Coronal CT demonstrating an oval fluid density below the right inferior pulmonary vein (*arrow*) consistent with pulmonary venous recess fluid (**a**). Axial CT showing a right pericardial fluid attenuation lesion (*arrow*) compatible with pericardial cyst (**b**). Anterior mediastinal well-circumscribed density

with soft-tissue attenuation (*arrow*), which was resected and identified as a thymic cyst on pathology (**c**). Low-attenuation oval lesion at the level of the aortic hiatus (*white arrow*) with communication with the thoracic duct (*black arrow*), characteristic for a cisterna chyli (**d**)

### 6.5.2 Cervical Rib

Cervical ribs are accessory ribs that articulate with the transverse process of the seventh cervical vertebrae [14, 15]. Its incidence in the general population is about 0.5%. Cervical ribs can be identified on chest radiograph as supernumerary ribs above the true ribs. Angiography with CT or MR is indicated to establish the anatomic rela-

tionship of the anomalous rib and adjacent vascular structure (Fig. 6.13). While most patients with cervical ribs are asymptomatic, thoracic outlet syndrome develops in a small percentage of cases due to compression of the subclavian vessels or brachial plexus. Symptoms of this syndrome include pain, weakness, decreased pulses, or swelling of the affected upper extremity.

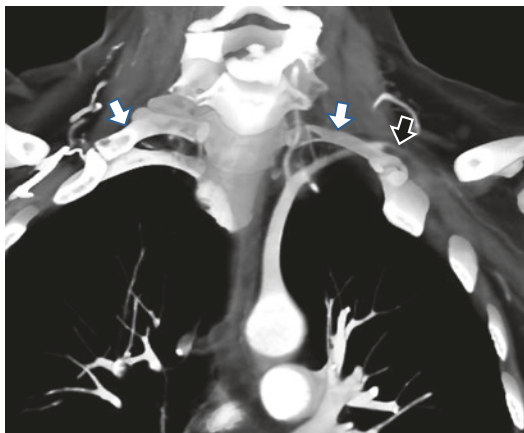


**Fig. 6.13** Coronal thick-slice maximum intensity projection image revealing bilateral cervical ribs (*arrows*), on the left causing occlusion of the subclavian artery (*arrow-head*). The cervical ribs articulate with bony processes protruding from the first ribs

### 6.5.3 Pectus Excavatum

Pectus excavatum (funnel chest) is the most common congenital deformity of the chest wall, occurring in approximately 1 in 700 births [16]. Abnormal growth and orientation of the lower costochondral cartilage are generally thought to be the etiology of pectus excavatum. The inferior sternum is depressed into a concave shape causing the ribs to protrude anteriorly. Pectus excavatum is readily diagnosed on lateral chest radiograph. Cross-sectional imaging demonstrates the severity of sternal depression and associated cardiac displacement (Fig. 6.14). Haller et al. developed the “pectus index” which is calculated by dividing the transverse diameter of the chest wall by the anteroposterior distance. He found that patients with pectus excavatum requiring surgery had an index  $>3.25$ , whereas normal control patients had a mean index of 2.56.

## 6.6 Thoracic Nerves

The brachial plexus comprises an arrangement of the C5–T1 nerves, responsible for sensorimotor innervation to the ipsilateral shoulder and upper extremity [17]. It travels alongside the subclavian artery and passes through the interscalene trian-



**Fig. 6.14** Axial CT image of a patient with Marfan syndrome. The anteroposterior distance between the sternum and the vertebral body is markedly decreased (*arrow*), diagnostic for pectus excavatum. Note the leftward displacement of the heart

gle—a space bordered by the anterior scalene muscle, the middle scalene muscle, and the first rib (Fig. 6.15). Due to its proximity to the lung apex, the brachial plexus is susceptible to invasion by superior sulcus tumor, also known as Pancoast tumor. Limited involvement of the brachial plexus may be amenable to surgical resection, whereas extensive tumor invasion of the brachial plexus remains a contraindication to surgery. The extent of brachial nerve and vascular involvement is best assessed using MRI techniques.

The phrenic nerve forms from the C3–C5 nerve roots and courses inferiorly to innervate the diaphragms. The paired phrenic nerves are located along the anterolateral mediastinum and pericardium, run parallel to pericardiophrenic arteries and veins, and arborize at the diaphragmatic surface (Fig. 6.15). Injury to the phrenic nerve is not uncommon due to invasive tumor or after cardiac surgery. Direct visualization of phrenic nerve injury is generally not possible with cross-sectional imaging. Chest fluoroscopy is an appropriate examination for establishing the diagnosis of diaphragmatic paralysis.

Awareness of the course of the recurrent laryngeal nerve (RLN) is important as damage to this nerve can occur anywhere along its course and lead to vocal cord paralysis. The right vagus nerve runs posterolateral to the common carotid arteries before giving off the right RLN, which

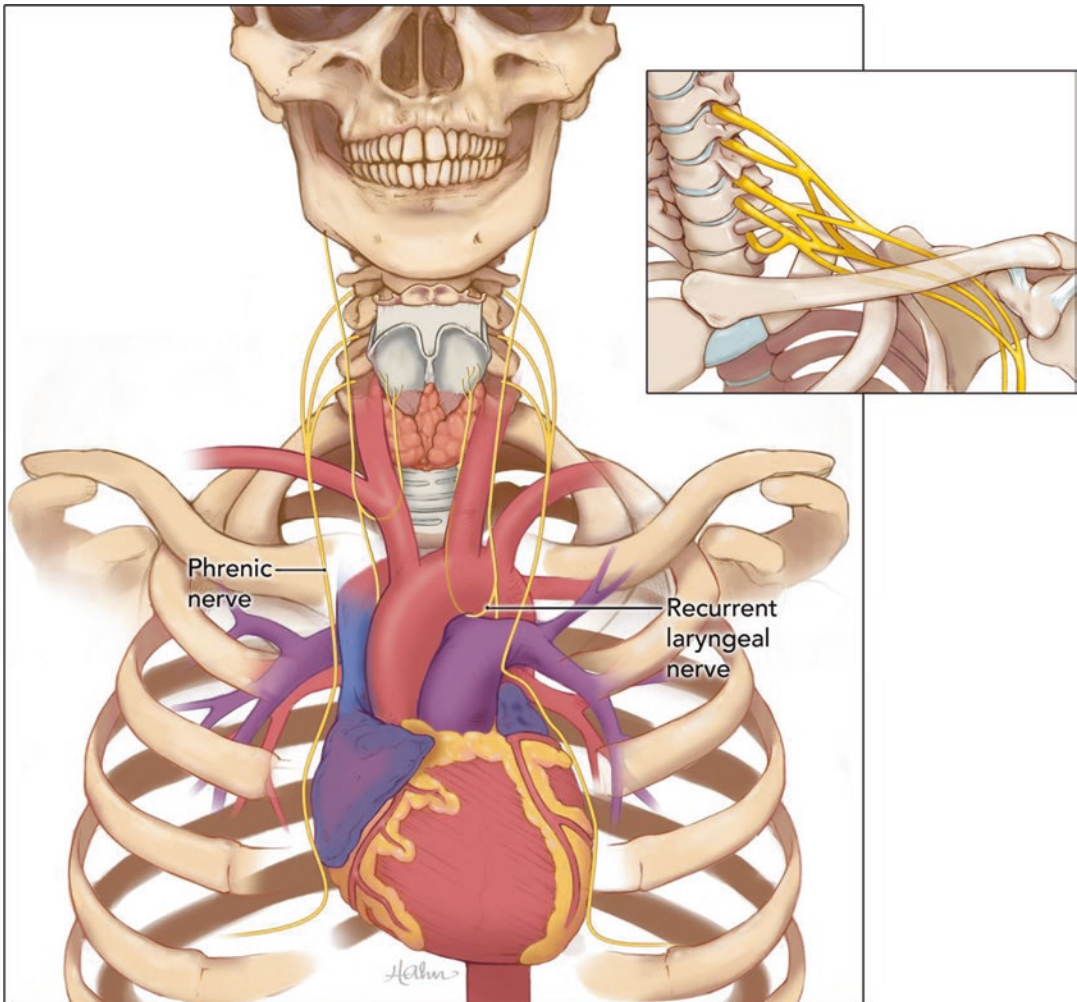


**Fig. 6.15** Illustration of the phrenic nerves, recurrent laryngeal nerves (RLNs), and brachial plexus (insert). Note the path of the left RLN between the aortic arch and pulmonary artery, while the right RLN courses under the right subclavian artery. Phrenic nerves follow the lateral

borders of the cardiomediastinal structures. The C5–T1 nerve roots form the branching network called the brachial plexus, coursing between the scalene muscles and under the clavicle

then travels posterior to the subclavian artery before moving to the larynx. The left RLN branches off from the vagus nerve at the aortopulmonary window and courses under the aortic arch posterior to the ligamentum arteriosum before ascending to the larynx. Therefore, in patients presenting with hoarseness concerning for vocal cord dysfunction, CT imaging should extend inferiorly to include the mediastinum.

## References

1. Davies M, Guest PJ. Developmental abnormalities of the great vessels of the thorax and their embryological basis. *Br J Radiol.* 2003;76:491–502.
2. Wooten C, Patel S, Cassidy L, et al. Variations of the tracheobronchial tree: anatomical and clinical significance. *Clin Anat.* 2014;27:1223–33.
3. Ghaye B, Szapiro D, Fanchamps JM, Dondelinger RF. Congenital bronchial abnormalities revisited. *Radiographics.* 2001;21:105–19.

4. Soto-Hurtado EJ, Penuela-Ruiz L, Rivera-Sanchez I, Torres-Jimenez J. Tracheal diverticulum: a review of the literature. *Lung*. 2006;184:303–7.
5. Aziz A, Ashizawa K, Nagaoki K, Hayashi K. High resolution CT anatomy of the pulmonary fissures. *J Thorac Imaging*. 2004;19:186–91.
6. Yildiz A, Golpinar F, Calikoglu M, Duce MN, Ozer C, Apaydin FD. HRCT evaluation of the accessory fissures of the lung. *Eur J Radiol*. 2004;49:245–9.
7. Applegate KE, Goske MJ, Pierce G, Murphy D. Situs revisited: imaging of the heterotaxy syndrome. *Radiographics*. 1999;19:837–52; discussion 53–4.
8. Jawad H, Sirajuddin A, Chung JH. Review of the international association for the study of lung cancer lymph node classification system: localization of lymph node stations on CT imaging. *Clin Chest Med*. 2013;34:353–63.
9. Truong MT, Erasmus JJ, Gladish GW, et al. Anatomy of pericardial recesses on multidetector CT: implications for oncologic imaging. *AJR Am J Roentgenol*. 2003;181:1109–13.
10. Jeung MY, Gasser B, Gangi A, et al. Imaging of cystic masses of the mediastinum. *Radiographics*. 2002;22:S79–93.
11. Kiyonaga M, Mori H, Matsumoto S, Yamada Y, Sai M, Okada F. Thoracic duct and cisterna chyli: evaluation with multidetector row CT. *Br J Radiol*. 2012;85:1052–8.
12. Feuerlein S, Kreuzer G, Schmidt SA, et al. The cisterna chyli: prevalence, characteristics and predisposing factors. *Eur Radiol*. 2009;19:73–8.
13. Restrepo CS, Martinez S, Lemos DF, et al. Imaging appearances of the sternum and sternoclavicular joints. *Radiographics*. 2009;29:839–59.
14. Kurihara Y, Yakushiji YK, Matsumoto J, Ishikawa T, Hirata K. The ribs: anatomic and radiologic considerations. *Radiographics*. 1999;19:105–19; quiz 51–2.
15. Guttentag AR, Salwen JK. Keep your eyes on the ribs: the spectrum of normal variants and diseases that involve the ribs. *Radiographics*. 1999;19:1125–42.
16. Jeung MY, Gangi A, Gasser B, et al. Imaging of chest wall disorders. *Radiographics*. 1999;19:617–37.
17. Aquino SL, Duncan GR, Hayman LA. Nerves of the thorax: atlas of normal and pathologic findings. *Radiographics*. 2001;21:1275–81.